

# Stabilizing G-Quadruplex DNA by a Scissors-Shaped Binaphthyl Derivative through the Entangling Mode: Cooperation of Binaphthylene and the Ethoxy Chain

Hong Zhang,<sup>‡,||</sup> Jun-feng Xiang,<sup>‡</sup> Hai-yu Hu,<sup>||,§</sup> Lin Li,<sup>‡,||</sup> Xue Jin,<sup>‡</sup> Yan Liu,<sup>‡</sup> Peng-fei Li,<sup>||,§</sup> Yalin Tang,<sup>\*,‡</sup> and Chuan-feng Chen<sup>\*,§</sup>

<sup>‡</sup>Beijing National Laboratory for Molecular Sciences, Center for Molecular Sciences, State Key Laboratory for Structural Chemistry of Unstable and Stable Species, <sup>§</sup>National Laboratory for Molecular Sciences, Center for Chemical Biology, and <sup>||</sup>Graduate University of the Chinese Academy of Sciences, Institute of Chemistry, Chinese Academy of Sciences, Beijing 100190, China

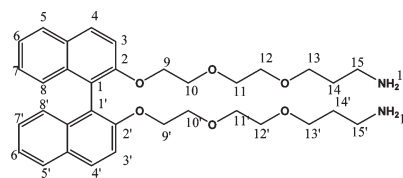
Received February 4, 2010; Revised Manuscript Received November 9, 2010

**ABSTRACT:** A scissors-shaped binaphthyl derivative (NPA) has been found to stabilize the G-quadruplex by intertwining the whole G-quadruplex with two long chains, through the cooperation of the two functional groups: binaphthylene and the ethoxy chain. Moreover, NPA exhibits a good inhibitory effect of telomerase activity as well as excellent cytotoxic activity against HepG-2 human liver cancer cells.

Telomerase is a cellular reverse transcriptase that maintains the integrity of the chromosome ends, the telomeres, to provide genomic stability in highly proliferating normal, immortal, and tumor cells. Active telomerase has been detected in a majority of tumor cells (>85%), while it is inactive in most somatic tissues, making it an attractive target for antitumor drug design, especially for cancer chemotherapy (1). Optimal telomerase activity requires an unfolded single-stranded telomeric overhang (2), which can form “quadruplex” structure with monovalent cations ( $K^+$  or  $Na^+$ ) (3). Therefore, ligands that can stabilize G-quadruplex structures may act as telomerase inhibitors (4). Recent investigation has shown that only a few of these ligands affect the processivity of telomerase, although they may lock telomerase substrates into a folded conformation leading to the initiation of elongation by telomerase. In fact, these ligands are more effective inhibitors of telomeric DNA amplification than extension by telomerase. These observations suggest that quadruplex ligands act as broad inhibitors of telomere-related processes, rather than simple telomerase inhibitors (5).

Recently, a number of molecules have been found binding to G-quadruplex DNA (6). Features shared by most of them include a large flat aromatic surface and an electron-deficient charge system (7). The planar aromatic chromophores are thought to be the key features (8). However, judging from the structures of G-quadruplexes, molecules can bind to the G-quadruplex through the face, edge, groove, or loop (9). Therefore, molecules with novel structures should be able to bind to G-quadruplexes. Actually, several G-quadruplex ligands without flat aromatic plane have been reported. For example, a carbocyanine dye, DODC, binds via a groove interaction, with one end projecting into the thymine loop region and stacking between the loop thymines and terminal guanine quartet (10). Moreover, several hemicyanine–peptide conjugates, derivatives of DODC, were found to bind to the G-quadruplex via loop and groove interactions (11). In addition, some macrocyclic molecules [telomestatin (12), HXDV (13), bistrioxazole

Scheme 1: Structural Formula of the NPA Molecule



acetate (14), and oxazole-based peptide macrocycles (15)] and small linear molecules [spermine (16), triethylene teraamine (17), distamycin A (18), and ethanol (19)] have shown a high affinity for binding to G-quadruplex DNA. These results strongly suggest a possibility to find G-quadruplex ligands with novel structures. Herein, we have found a scissorslike molecule, 3-(2-{2-[1-(2-{2-(3-aminopropoxy)ethoxy}ethoxy)naphthalen-1-yl]naphthalen-2-yloxy}ethoxy)ethoxy)propan-1-amine (NPA) (Scheme 1), can also stabilize G-quadruplexes. Surprisingly, only cooperation of two groups, binaphthanyl (BINOL) and the amino-terminated poly(ethylene glycol) chain (PEG-NH<sub>2</sub>), could bind to G-quadruplex structure. Further two-dimensional (2D) NMR results show the NPA molecule binds to the G-quadruplex in the entangling mode.

The ability of NPA, BINOL, and PEG-NH<sub>2</sub> to stabilize G-quadruplex DNA was then investigated by temperature-dependent UV measurement in the presence of PBS-K<sup>+</sup> (20, 21). Our results have shown that NPA could stabilize intramolecular [Hu24-(TTAGGG)<sub>4</sub>, Hu24A-TTGGG(TTAGGG)<sub>3</sub>A, and Hu22-AGGG(TTAGGG)<sub>3</sub>] and intermolecular {Hu7-[d(TTAGGGT)]<sub>4</sub>} G-quadruplex structures by increasing the melting temperature ( $\Delta T_m$ ) by 4–9 °C while BINOL and PEG-NH<sub>2</sub> do not (Table S1 of the Supporting Information), suggesting a possible cooperation of these two functional groups in stabilizing G-quadruplex structure. Such interesting results prompt us to further investigate how this scissors-shaped NPA molecule stabilizes the G-quadruplex. Thus, we have conducted NMR experiments to investigate the interaction between NPA and intermolecular parallel-stranded quadruplex Hu7 because this quadruplex exhibits well-resolved NMR signals with full assignments (22–24).

Figure 1 shows the <sup>1</sup>H NMR spectra of Hu7 in the 11–12 ppm region with three well-resolved signals assigned to G4, G5, and G6. Surprisingly, addition of NPA to Hu7 results in progressive downfield shifts of these NMR signals. Clearly, these changes are greatly different from those of the known G-quadruplex ligands with a planar aromatic ring for which these signals shift upfield upon addition of ligands. For example, binding with TmPyP4 induced the upfield shifts of G4–G6 proton signals because of the ring current effect (25). Similar behaviors have been observed

\*To whom correspondence should be addressed. Telephone: 0086-10-6252-2090. Fax: 0086-10-8261-7302. E-mail: tangyl@iccas.ac.cn (Y.T.) or cchen@iccas.ac.cn (C.-f.C.).

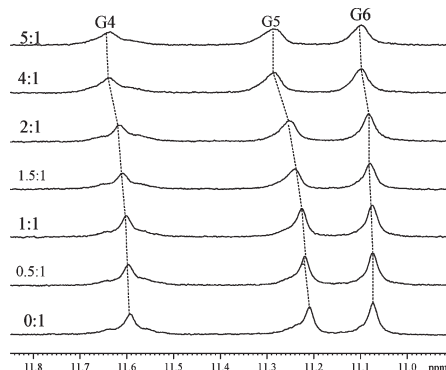


FIGURE 1: <sup>1</sup>H NMR spectra recorded in the 30% DMSO/70% H<sub>2</sub>O (v/v) solution showing the imino proton resonances for G4, G5, and G6 in **Hu7** with various molar ratios of NPA.

for other molecules, PIPER (26), RHPS4 (27), and quercetin (28), with similar structural features. Therefore, these results indicate NPA should exhibit a different mode of binding to the G-quadruplex.

Compared with chemical shift changes of G4 and G6 with the increase in NPA concentration, the largest changes were observed for G5, suggesting that the NPA molecule binds to **Hu7** much closer to G5 than to G4 and G6. Furthermore, judged from the titration results, NPA and **Hu7** could form a 4:1 complex (Figure S4 of the Supporting Information) because the resonances of the imino protons nearly remain unchanged when the NPA concentration is more than 4 equiv of the **Hu7** concentration. Moreover, the results of CD titrations (29) (Figures S5 and S6 of the Supporting Information) also show a similar tendency, which is consistent with the NMR titration results.

To gain more information about the interactional mode between NPA and **Hu7**, we measured the 2D NMR intermolecular NOESY (Figure 2) and TOCSY (Figure S7 of the Supporting Information) spectra. Three new NOEs were detected clearly except for the known correlation peaks (Figure 2a). The G6NH peak at 11.11 ppm exhibits NOEs to the base protons of G6H8 and G5H8, and the connective peaks between the 4,4' and 3,3' protons of the NPA were also observed. The imino proton of G5 at 11.29 ppm exhibits NOEs with not only the base proton of G5H8 and G4H8 but also the 4,4' proton of NPA. From Figure 2b, the weak but clear NOE cross-peaks of the 9,9' proton with G6H8, G4H8, and T2H6 were observed. Additionally, the cross-peaks of the 3,3' proton with T1H6, T2H6, A3H2, and G6H8 and the 4,4' proton with G6H8 and T7H6 were detected (Figure 2c). These results suggested that NPA is bound to **Hu7** from T1 to T7, when the molar ratio of NPA to the G-quadruplex is 4:1.

Compared with the compounds with amino-terminal side chains (15), these primary amines may specifically interact with the negatively charged backbone phosphates of G-quadruplex grooves, which help stabilize G-quadruplex. On the basis of the titration results, the chemical shifts of proton signals of **Hu7** are ranked in the following order: T7CH3 > T2H6 > G5 > G4 > G6 > A3H8 > T1CH3 (when the molar ratio of NPA to **Hu7** varied from 0:1 to 5:1) (Figure S4 of the Supporting Information). The largest changes in both T7 and T2 could be attributed to the binding to the negatively charged phosphate backbone of the G-quadruplex. Combined with the binding mode described above (Figure S8 of the Supporting Information), these results indicated that NPA binds to the G-quadruplex via entangle binding.

Further molecular modeling results (Figure S9 of the Supporting Information) show that the molecular size of NPA can be

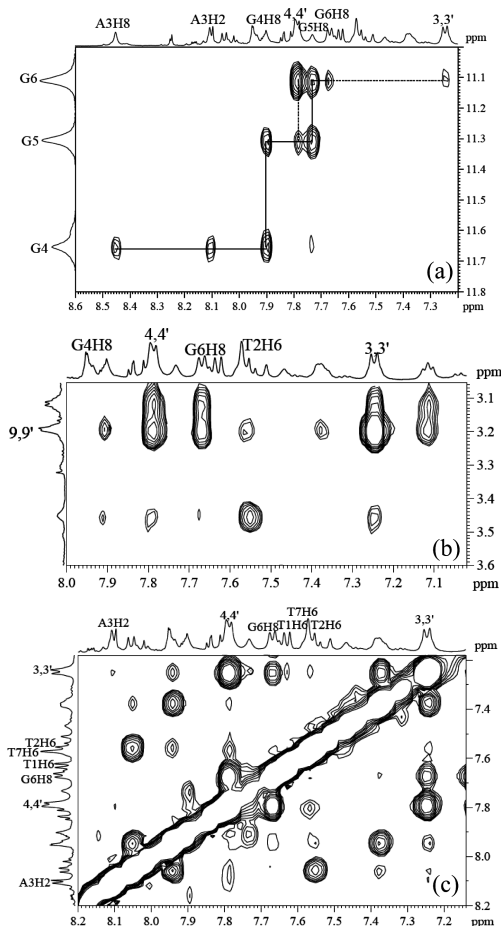


FIGURE 2: Portion of the 2D NOESY spectrum of the 4:1 NPA–**Hu7** complex recorded at 298 K with a mixing time of 0.3 s. (a) GN1–H NOE base H6/H8 stacking between G- and A-tetrads (—) and cross-peaks between NPA and G5 and G6 (···). (b) Connectivity between the 9,9' proton of two chain resonances and **Hu7**. (c) Connectivity between the 3,3' and 4,4' protons of binaphthanyl resonances and **Hu7**.

perfectly fit to the size of the quadruplex groove. For example, the lengths of the quadruplex from G5 to T7 and from T2 to G4 are 12.6 and 12.7 Å, respectively. The length of the ether chain is 12.2 Å. When the molar ratio of NPA to the G-quadruplex is 4:1, the side chains of two adjacent NPA molecules could just match the length of the G-quadruplex groove. However, the competitive FRET results (Figure S10 and Table S2 of the Supporting Information) have shown that the NPA molecule appears to be less competent because the  $\Delta T_m$  value is sensitive to the duplex competition, suggesting that NPA might not be a good G-quadruplex ligand.

As mentioned above, small molecules that stabilize the G-quadruplex structure might act as telomerase inhibitors. Therefore, the inhibition of telomerase activity of NPA has been evaluated by using both a classical telomere repeat amplification protocol (TRAP) assay (29) and a modified TRAP-LIG assay (30). Figure 3 shows the inhibiting ability of NPA in both assays. The classical TRAP assay revealed a dose-dependent inhibition of the telomerase ladder, starting at 0.06  $\mu$ M and ending at 0.08  $\mu$ M, while telomerase inhibition occurred at 0.1–0.3  $\mu$ M NPA by using the modified TRAP-LIG assay. These results suggested that the telomerase inhibition activity of the NPA molecule might be overestimated by using the classical TRAP assay. More importantly, the TRAP results suggest that NPA is a potential telomerase inhibitor, although it exhibits only moderate stability of G-quadruplexes.

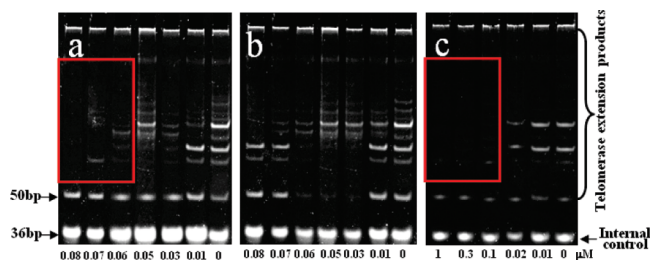


FIGURE 3: Inhibition of telomerase activity by the NPA molecule with a classical (a) and a modified TRAP assay (b and c). Typical products of telomerase activity are shown by the bands starting from 50 bp, and the internal control results in a single band of 36 bp. The red boxed areas show the progressive decrease in the intensity of the ladder (i.e., increase in the level of telomerase inhibition).

Finally, the cytotoxic activities of these three compounds (NPA, BINOL, and PEG-NH<sub>2</sub>) were determined by using an MTT assay (Figure S12 of the Supporting Information). NPA exhibits a 100% suppression ratio against HepG-2 human liver cancer cells even though the concentration is as low as 0.1  $\mu$ M, while both BINOL and PEG-NH<sub>2</sub> exhibit no suppression ratios. This result, together with TRAP-LIG assay, suggested that the cytotoxicity of this novel molecule may result from its role in telomerase inhibition.

In summary, a novel scissors-shaped molecule NPA has been shown to increase the melting temperature of the quadruplex by the entangling mode, which may be attributed to the cooperation of binaphthylene and the amino-terminated ethoxy chain in the NPA molecule. Moreover, the NPA molecule exhibits an excellent telomerase inhibition and cytotoxic activity. The novel molecular structure may offer us a hint about constructing new anticancer agents.

## ACKNOWLEDGMENT

This work is supported by the National Natural Science Foundation of China (20625206 and 81072576).

## SUPPORTING INFORMATION AVAILABLE

Details for <sup>1</sup>H NMR, TOCSY, synthesis of NPA and PEG-NH<sub>2</sub>, absorption measurement, FRET, CD titrations, molecular model, MTT, and TRAP. This material is available free of charge via the Internet at <http://pubs.acs.org>.

## REFERENCES

1. Harley, C. B. (2008) *Nature* 8, 167–179.
2. Zahler, A. M., Williamson, J. R., Cech, T. R., and Prescott, D. M. (1991) *Nature* 350, 718–720.

3. Salazar, M., Thompson, B. D., Kerwin, S. M., and Hurley, L. H. (1996) *Biochemistry* 35, 16110–16115.
4. De Cian, A., Lacroix, L., Douarre, C., Temime-Smaali, N., Trentesaux, C., Riou, J. F., and Mergny, J. L. (2008) *Biochimie* 90, 131–155.
5. De Cian, A., Cristofari, G., Reichenbach, P., De Lemos, E., Monchaud, D., Teulade-Fichou, M. P., Shin-ya, K., Lacroix, L., Lingner, J., and Mergny, J. L. (2007) *Proc. Natl. Acad. Sci. U.S.A.* 104, 17347–17352.
6. Monchaud, D., and Teulade-Fichou, M. P. (2008) *Org. Biomol. Chem.* 6, 627–636.
7. Ou, T., Lu, Y., Tan, J., Huang, Z., Wong, K., and Gu, L. (2008) *ChemMedChem* 3, 690–713.
8. Mergny, J. L., Lacroix, L., Teulade-Fichou, M. P., Hounsou, C., Guittat, L., Hoarau, M., Arimondo, P. B., Vigneron, J. P., Lehn, J. M., Riou, J. F., Garestier, T., and Helene, C. (2001) *Proc. Natl. Acad. Sci. U.S.A.* 98, 3062–3067.
9. Davis, J. T. (2004) *Angew. Chem., Int. Ed.* 43, 668–698.
10. Chen, Q., Kuntz, I. D., and Shafer, R. H. (1996) *Proc. Natl. Acad. Sci. U.S.A.* 93, 2635–2639.
11. Schouten, J. A., Ladame, S., Mason, S. J., Cooper, M. A., and Balasubramanian, S. (2003) *J. Am. Chem. Soc.* 125, 5594–5595.
12. Kim, M. Y., Vankayalapati, H., Shin-ya, K., Wierzba, K., and Hurley, L. H. (2002) *J. Am. Chem. Soc.* 124, 2098–2099.
13. Barbieri, C. M., Srinivasan, A. R., Rzuczek, S. G., Rice, J. E., LaVoie, E. J., and Pilch, D. S. (2007) *Nucleic Acids Res.* 35, 3272–3286.
14. Tera, M., Sohtome, Y., Ishizuka, H., Doi, T., Takagi, M., Shin-ya, K., and Nagasawa, K. (2006) *Heterocycles* 69, 505–514.
15. Jantos, K., Rodriguez, R., Ladame, S., Shirude, P. S., and Balasubramanian, S. (2006) *J. Am. Chem. Soc.* 128, 13662–13663.
16. Keniry, M. A., and Owen, E. A. (2007) *Eur. Biophys. J.* 36, 637–646.
17. Yin, F., Liu, J., and Peng, X. (2003) *Bioorg. Med. Chem. Lett.* 13, 3923–3926.
18. Martino, L., Virno, A., Pagano, B., Virgilio, A., Micco, S. D., Galeone, A., Giancola, C., Bifulco, G., Mayol, L., and Randazzo, A. (2007) *J. Am. Chem. Soc.* 129, 16048–16056.
19. Vorlickova, M., Bednarova, K., and Kypr, J. (2006) *Biopolymers* 82, 253–260.
20. Rachwal, P. A., and Fox, K. R. (2007) *Methods* 43, 291–301.
21. Guedin, A., De Cian, A., Gros, J., Lacroix, L., and Mergny, J. L. (2008) *Biochimie* 90, 686–696.
22. Gavathiotis, E., and Searle, M. S. (2003) *Org. Biomol. Chem.* 1, 1650–1656.
23. Gavathiotis, E., Heald, R. A., Stevens, M. F. G., and Searle, M. S. (2003) *J. Mol. Biol.* 334, 25–36.
24. Hounsou, C., Guittat, L., Monchaud, D., Jourdan, M., Saettel, N., Mergny, J. L., and Teulade-Fichou, M. P. (2007) *ChemMedChem* 2, 655–666.
25. Mita, H., Ohyama, T., Tanaka, Y., and Yamamoto, Y. (2006) *Biochemistry* 45, 6765–6772.
26. Fedoroff, O. Y., Salazar, M., Han, H., Chemeris, V. V., Kerwin, S. M., and Hurley, L. H. (1998) *Biochemistry* 37, 12367–12374.
27. Gavathiotis, E., Heald, R. A., Stevens, M. F. G., and Searle, M. S. (2001) *Angew. Chem., Int. Ed.* 40, 4749–4751.
28. Sun, H., Tang, Y., Xiang, J., Xu, G., Zhang, Y., Zhang, H., and Xu, L. (2006) *Med. Chem. Lett.* 16, 3586–3589.
29. De Cian, A., Delemos, E., Mergny, J. L., Teulade-Fichou, M. P., and Monchaud, D. (2007) *J. Am. Chem. Soc.* 129, 1856–1857.
30. Reed, J., Gunaratnam, M., Beltran, M., Reszka, A. P., Vilar, R., and Neidle, S. (2008) *Anal. Biochem.* 380, 99–105.